



# Enhanced thermal conductivity and long-term stability of diamond/aluminum composites using SiC-coated diamond particles

Emin Kondakci<sup>1</sup> and Nuri Solak<sup>1,2,\*</sup>

<sup>1</sup>Department of Metallurgical and Materials Engineering, Istanbul Technical University, 34469 Istanbul, Turkey

<sup>2</sup>Center for Critical and Functional Materials, Istanbul Technical University, 34469 Istanbul, Turkey

Received: 20 July 2021

Accepted: 13 December 2021

Published online:

3 January 2022

© The Author(s), under exclusive licence to Springer Science+Business Media, LLC, part of Springer Nature 2021

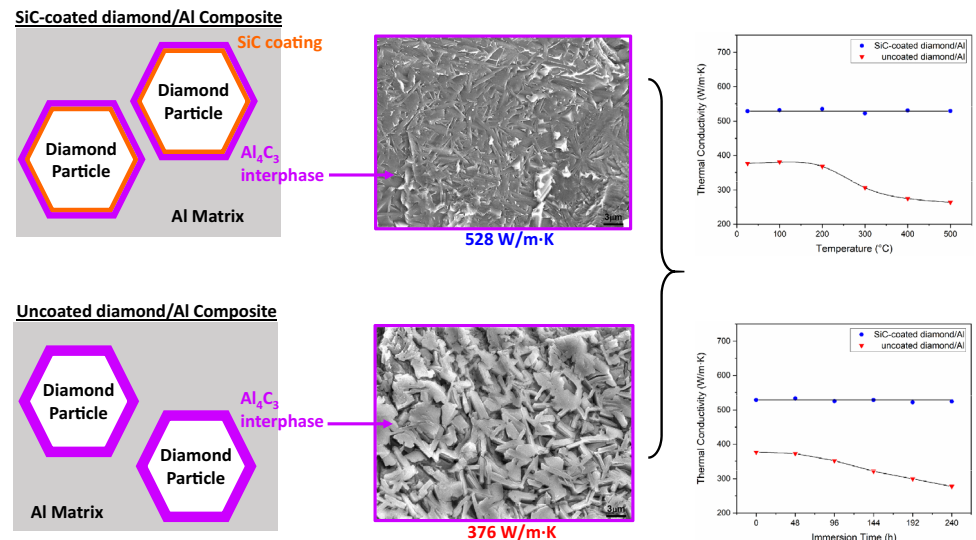
## ABSTRACT

In this study, diamond/aluminum composites were fabricated by the use of gas pressure infiltration. The effects of SiC-coated diamond particles on composite performance were investigated in terms of: (1) controlling the thermal conductivity (TC) during composite fabrication and (2) providing long-term stability.  $Al_4C_3$  spontaneously forms at the interface of the diamond particles and the Al matrix. An excess amount of  $Al_4C_3$  interphase adversely affects the composite, due to its low TC and hygroscopic behavior. Because the SiC coating of diamond particles suppressed the formation of  $Al_4C_3$  during the fabrication, the composite contained a low amount of  $Al_4C_3$  and showed higher a TC (528 W/m·K) than uncoated diamond/Al composite (376 W/m·K), along with significantly higher moisture resistance. The thermal expansion coefficient (CTE) of the SiC-coated diamond/Al composite was determined to be 7.2 ppm/K at room temperature. The composite exhibited long-term stability up to 500 °C as the Al-C reaction was prevented by the SiC coating. Moreover, it displayed excellent thermal shock resistance between 300 °C and room temperature.

Handling Editor: N. Ravishankar.

Address correspondence to E-mail: solaknu@itu.edu.tr

## GRAPHICAL ABSTRACT



## Introduction

With increasing miniaturization and improvement in components, advances in microelectronics technology have led to increased power density and consequent higher heat flux in integrated circuits. Overheating of electronic components decreases their performance and reliability. For example, a *ca.* 10 °C increase in temperature reduces the average failure time of microchips by a factor of two. Because the state of the art in IC chip fabrication is presently at 7 nm, heat dissipation plays an especially pivotal role, via heat sinks with even higher thermal conductivity (TC). In addition to high TC, the coefficient of thermal expansion (CTE) of thermal management materials must be compatible with adjacent electronic components. Mismatch in CTE results in thermal stress-induced failure of joints due to thermal stress and slower dissipation of the heat released. Other requirements for advanced thermal management materials are long-term TC stability and low density [1–3].

Monocrystalline diamond has outstanding thermal properties well suited for such applications: high TC

(1200–2200 W/m·K) and low CTE ( $\sim 1$  ppm/K) [4, 5]. Therefore, monocrystalline diamond-reinforced metal-matrix composites such as diamond/aluminum (Al), diamond/copper, diamond/silver have been studied as new generation thermal management materials. Due to its light weight, relatively high oxidation resistance and lower cost, Al is a suitable matrix material.

The TC of diamond/Al composites mainly depends on the diamond quality (shape and TC), the diamond volume fraction, the Al content and the amount of interfacial phases [6–9]. Al<sub>4</sub>C<sub>3</sub> is the main phase formed at the interface as a result of the reaction between diamond particles and Al matrix. While the reaction contributes to TC by forming chemical bonds between the diamond particles and the Al matrix, an excess amount of Al<sub>4</sub>C<sub>3</sub> adversely affects the thermal properties, due to its low TC and hygroscopic behavior [9–14].

During the fabrication of diamond/Al composites, the amount of Al<sub>4</sub>C<sub>3</sub> interphase is mainly controlled by: (1) precise optimization of fabrication parameters [9, 15–17], (2) alloying of the Al matrix such as Si, Ti [8, 9, 18, 19] and (3) coating of diamond particles such as SiC, TiC, ZrC, W [10, 11, 20–22]. The common

purpose of all these methods is to suppress the reaction kinetics for forming  $\text{Al}_4\text{C}_3$  to enhance TC. Although previous studies reported in the literature have been focused on controlling of  $\text{Al}_4\text{C}_3$  formation during the composite fabrication, thermal management composites are exposed to heat and moisture under service conditions. Therefore, to achieve long-term TC stability, the method applied should also prevent the formation of  $\text{Al}_4\text{C}_3$  under service conditions and contribute to resistance of the composite against thermal shock and moisture.

We hypothesize that designing a high-performance diamond/Al metal–matrix composite should address simultaneously reaction control during fabrication and the long-term stability. SiC-coated diamond particles are known to offer higher TC compared to other carbide coatings, slower reaction kinetics with liquid Al and thermodynamic stability in contact with solid Al [11, 23, 24].

Prior works have shown that the SiC coating of diamond particles suppresses  $\text{Al}_4\text{C}_3$  formation during the fabrication of diamond/Al composites [11, 20]. However, in these studies, the long-term TC stability of SiC-coated diamond/Al composites has not been investigated in detail. It was concluded that the SiC-coated diamond/Al composites are stable in wet environments compared to the uncoated diamond/Al composite. No further TC stability tests were performed in the literature. So, it is necessary to clarify the effect of temperature on the TC stability of the composites.

In this study, SiC-coated diamond/Al composites were fabricated by use of gas pressure infiltration and irregular-shaped diamond particles, unlike previous reports in the literature. The effects of a SiC coating on the diamond particles were evaluated on the microstructure, thermal characteristics and TC stability tests. Thermal durability, thermal shock and wet environment durability tests were performed for the evaluation of the long-term stability of composites. The primary purpose of this work is to investigate the effects of SiC-coated diamond particles in terms of: (1) controlling the  $\text{Al}_4\text{C}_3$  interphase formation during composite fabrication and (2) providing long-term stability.

## Experimental details

### Materials

The starting materials were aluminum with the purity of 99.9 wt% as the matrix and synthetic monocrystalline diamond particles with an average particle size of  $D_{50} = 152 \mu\text{m}$  as the reinforcement. Synthetic diamond particles of lower cost and irregular shape (typically used in abrasive industry), as shown in Fig. 1a, were used to demonstrate that the effect of diamond quality on TC can be minimized by controlling the amount of  $\text{Al}_4\text{C}_3$  interphase. The diamond particles were coated with SiC by a reactive conversion method [25]. The XRD pattern of SiC-coated diamond particles is shown in Fig. 1b. The characteristic SiC (JCPDS 006-0675) and diamond

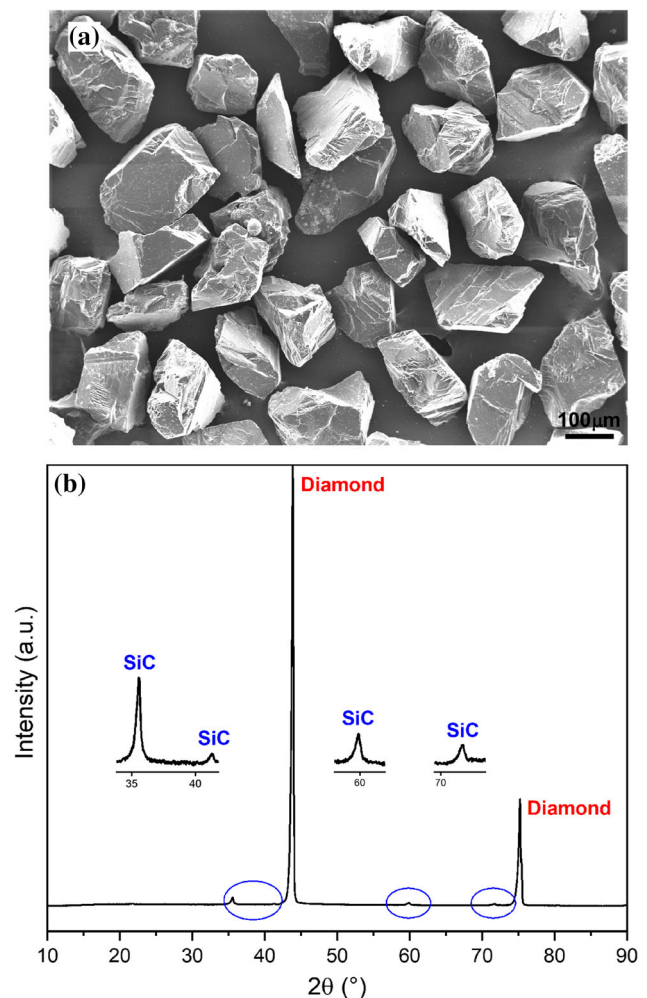


**Figure 1** a SEM image of the SiC-coated diamond particles, b XRD result of the SiC-coated diamond particles.

(JCPDS 029-1129) peaks were detected in the diffractogram.

### Fabrication process

The SiC-coated diamond/Al composites were fabricated by use of gas pressure infiltration and compared with control samples prepared with uncoated diamond particles. The diamond particles were densely packed into graphite molds, and a solid piece of Al was placed on the top of the particle beds. The assembly was then placed in a cold-wall infiltration furnace. The furnace was heated up to 800 °C at a rate of 10 °C/min by an induction heater. The melting of Al was performed at a vacuum level of better than 0.5 mbar to avoid oxidation. After reaching the infiltration temperature, the furnace was pressurized to 20 bar using high-purity argon gas to infiltrate molten Al into the free volume between diamond particles. The induction heating was switched off 15 min. After pressurization, it is followed by furnace cooling down to 300 °C while maintaining the same gas pressure. Upon reaching 300 °C, the gas was evacuated. The composites were infiltrated in a net shape of the dimensions required for thermal measurements.

### Characterization

TC of the composites was derived from the equation  $TC = T_{diff} \cdot \rho \cdot C_p$ , where  $T_{diff}$  is thermal diffusivity,  $\rho$  is bulk density and  $C_p$  is specific heat capacity. The thermal diffusivity was measured by the laser flash

technique (Netzsch LFA 457 Micro Flash) with an accuracy of  $\pm 3\%$ , using a disk composite with 12.5 mm in diameter and 3 mm in thickness. Diffusivity values were obtained from averaging of 10 measurements for each composite. Oxygen-free high-conductivity copper (OFHC) served as the reference. Density of the composites was determined by the Archimedes method using distilled water as the immersion medium. The density results were calculated from an average of 5 consecutive measurements. The specific heat capacity was determined by a differential scanning calorimeter (Netzsch STA 449 F3 Jupiter) with a heating rate of 1 °C/min up to 200 °C, with an accuracy of  $\pm 1.5\%$ . For the CTE measurements, a pushrod dilatometer (Netzsch DIL 402 Expedit) was used over the temperature range of 40 °C to 200 °C with a heating rate of 5 °C/min. The measurement was conducted under an argon atmosphere on a cylindrical composite sample of 4 mm in diameter and 10 mm in length. The room temperature CTE value was determined by extrapolation using the corresponding plot. Microstructural characterization was performed by using a field-emission scanning electron microscope (FE-SEM; JEOL JSM 7000F). The phase analyses were conducted by X-ray diffractometer (XRD; Panalytical Aeris) with Cu-K $\alpha$  radiation. A micro-Raman spectrophotometer with a 632.8 nm wavelength He/Ne laser (LabRam 800 Horiba Scientific Jobin-Yvon) was used to determine the presence of Al<sub>4</sub>C<sub>3</sub> interphase on the fracture surface of composites.

### The thermal conductivity stability tests

The TC stability tests were performed to investigate the effect of SiC-coated diamond particles on the composites under service conditions. Three types of tests were applied: thermal durability, thermal shock and wet environment durability. The thermal durability tests were conducted on the same sample consecutively at 100, 200, 300, 400, 500 °C, with the heating and cooling rates of 3 °C/min in air. The holding time was held constant for 1 h at each temperature. The uncoated diamond/Al composites were detrimentally affected during the test. To determine TC stability of SiC-coated diamond/Al composites at high temperature, the samples were subjected to an additional thermal durability test at 500 °C for 120 h. The thermal shock cyclic tests were performed from 300 °C to room temperature, by air

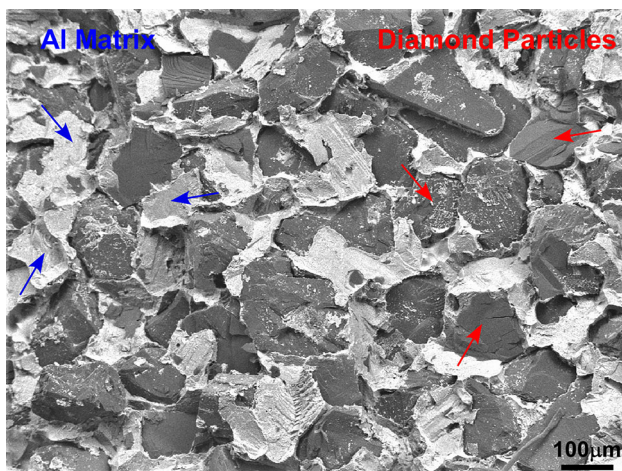


**Figure 2** Fractured surface BSE-SEM image of the SiC-coated diamond/Al composite.

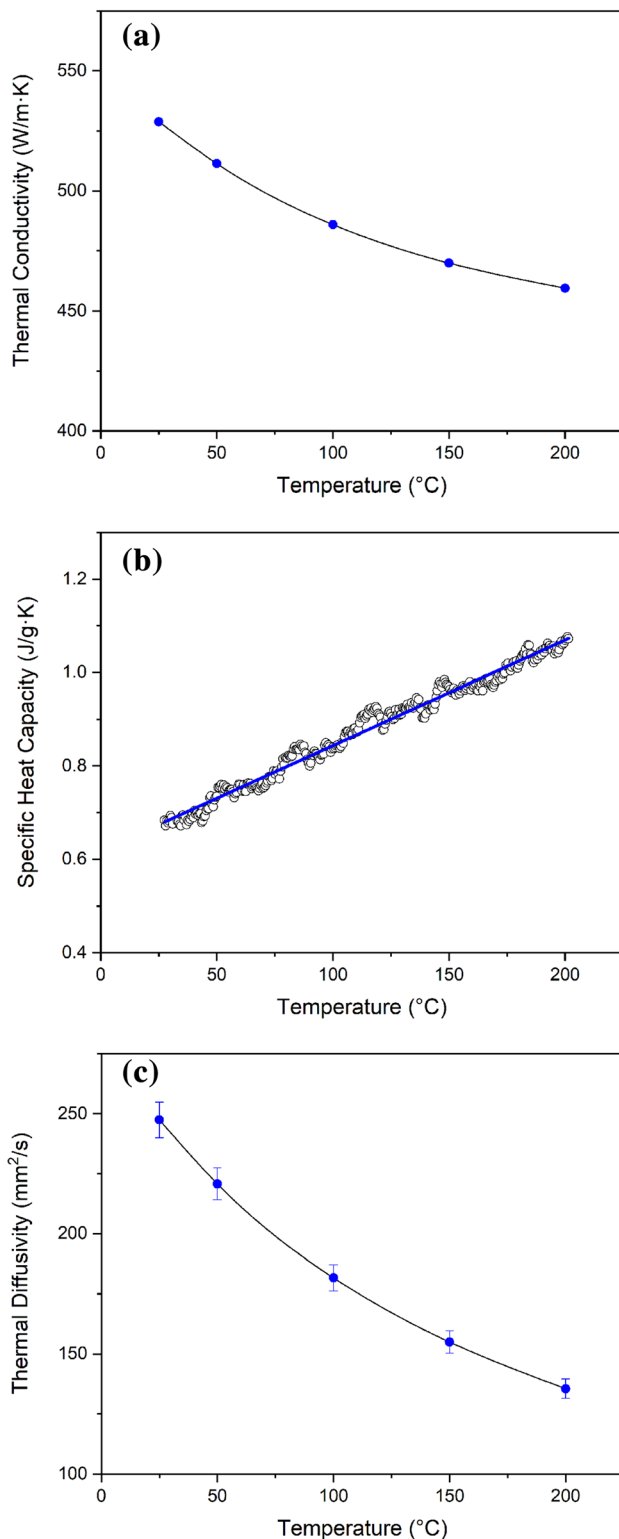


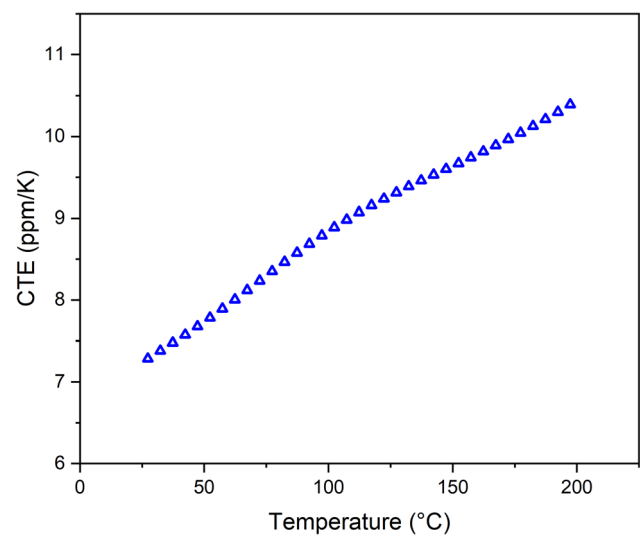
**Figure 3** a Thermal conductivity, b specific heat capacity and c thermal diffusivity results of the SiC-coated diamond/Al composite.

quenching, with a holding time of 15 min at each temperature. Wet environment durability tests were carried out in 100 ml of distilled water at room temperature for 240 h. To accelerate the effect of moisture, the composites were immersed into distilled water. All tests were done with three repetitions.

## Results and discussion

The fractured surface SEM image of the SiC-coated diamond/Al composite is shown in Fig. 2. The diamond particles were distributed homogeneously in the aluminum matrix. No porosity was observed in the matrix. The density of composites was measured as  $3.17 \pm 0.02 \text{ g/cm}^3$ , indicating an approximately 58% volume fraction of diamond. Particle geometry is one of the parameters that affected the diamond ratio in the mold. Since the diamond particles were significantly different from spherical shape, packing became difficult, and this led to a decrease in the density.

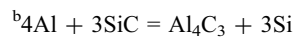
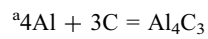
TC results of the SiC-coated diamond/Al composite were plotted as a function of temperature between room temperature and 200 °C (Fig. 3a). The values of TC were derived from its specific heat capacity (Fig. 3.b), thermal diffusivity (Fig. 3.c) and density. The TC of composite was obtained as 528 W/m·K at room temperature and decreased



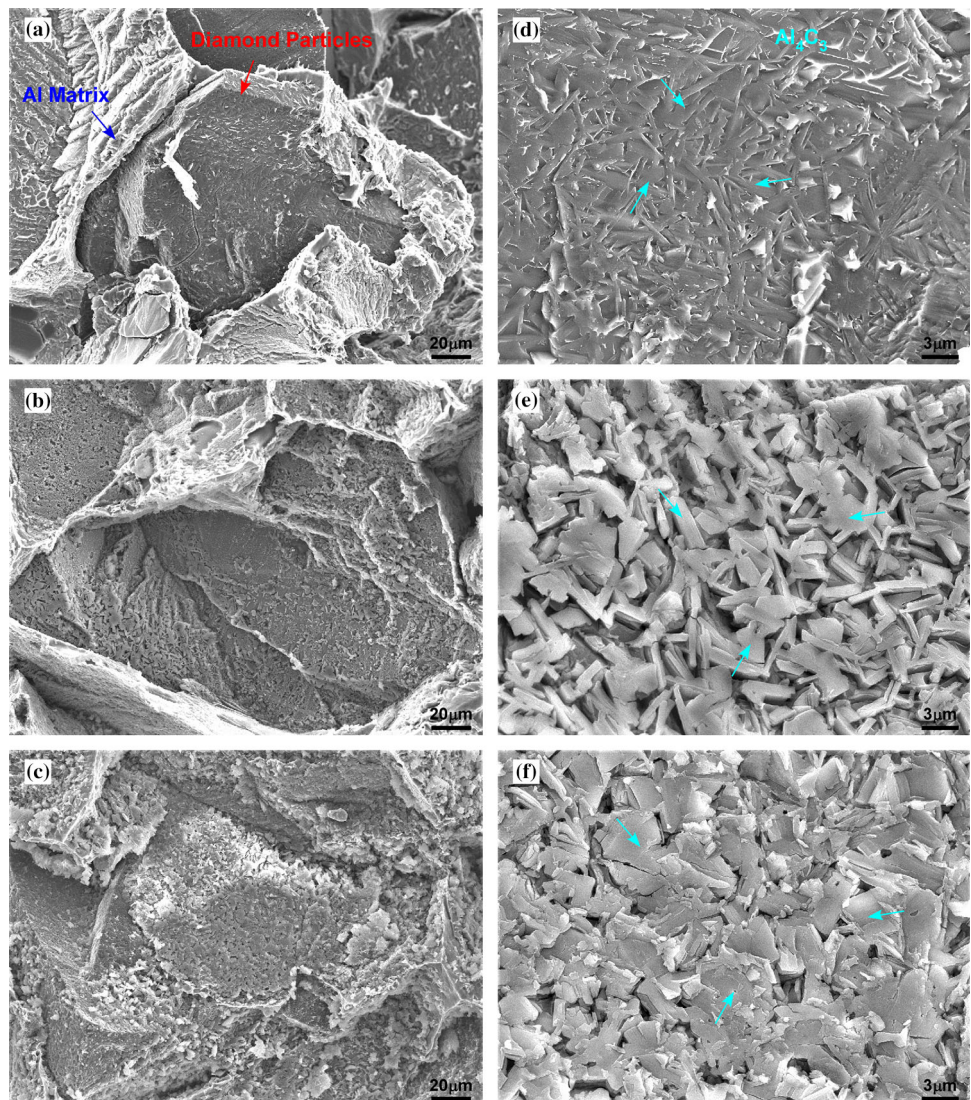
**Figure 4** Coefficient of thermal expansion results of the SiC-coated diamond/ Al composite.

**Table 1** Gibbs free energy change values of the reactions [28]

Temperature (°C)	Gibbs Free Energy Change <sup>a</sup> (kJ)	Gibbs Free Energy <sup>b</sup> (kJ)
0	– 240.39	4.70
100	– 200.23	6.41
200	– 196.02	8.16
300	– 191.80	9.94
400	– 187.52	11.79
500	– 183.14	13.75
600	– 178.61	15.87
700	– 172.04	20.02
800	– 162.55	27.08
900	– 152.95	34.24
1000	– 143.27	41.48



**Figure 5** Fractured surface SEM images of **a** the SiC-coated diamond/Al composite as-fabricated, **b** the uncoated diamond/Al composite as-fabricated and **c** the uncoated diamond/Al composite after thermal durability test. **d–f** high magnification of **a–c**, respectively.



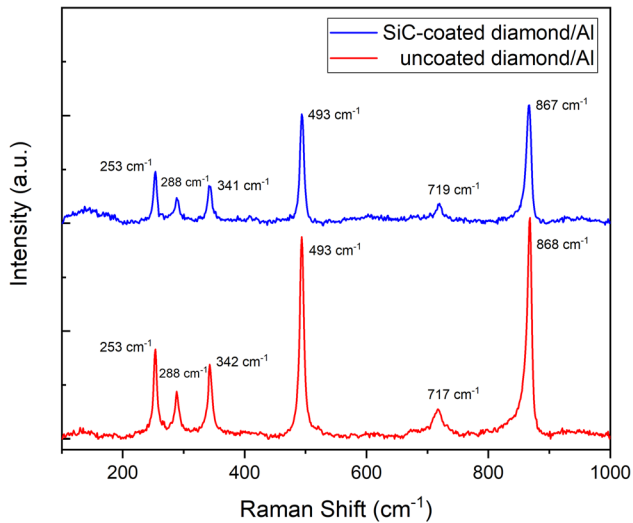


**Figure 6** Raman spectra of  $\text{Al}_4\text{C}_3$  interphase on the fracture surface of composites.

exponentially with the increasing temperature by Eq. (1). In fact, the SiC-coated diamond/Al composite provided a TC of above  $450 \text{ W/m}\cdot\text{K}$  up to  $200 \text{ }^\circ\text{C}$ . The TC values are significantly large compared to those in the literature for diamond/Al composites, despite the use of low-quality diamond particles.

$$\text{TC}(T) = 441 + 110 \left( \frac{-T}{112} \right), \quad R^2 = 1 \quad (1)$$

CTE results of the SiC-coated diamond/Al composite are shown in Fig. 4, between room temperature and  $200 \text{ }^\circ\text{C}$ . The CTE of the composite was determined as  $7.2 \text{ ppm/K}$  at room temperature. Such a CTE value indicates suitability for thermal management applications [3, 18, 19, 26, 27].

During the infiltration process, the molten Al reacts with the uncoated diamond particles, and  $\text{Al}_4\text{C}_3$  is formed at the interface due to the high reactivity and low solubility of carbon in Al. The reaction between Al and C is given in Eq. (2). However, the interfacial reaction for SiC-coated diamond/Al composite is governed by the reaction given in Eq. (3). Because the diamond particles are completely covered with SiC, the reaction between Al and SiC is responsible for the interphase formation, rather than the Al-C reaction. According to thermodynamic calculations [28], given in Table 1, the Gibbs free energy change ( $\Delta G_T$ ) of the reaction is positive-valued above the melting point of Al, indicating that SiC and liquid Al are thermodynamically in equilibrium. On the other hand, elemental silicon, which is the other reaction product, is

miscible in liquid Al, according to the Al-Si phase diagram. The decreased activity of silicon results in a negative  $\Delta G_T$ . Therefore, the reaction proceeds spontaneously. However, the reaction tends to terminate rapidly as the amount of dissolved silicon increases [23, 24, 29].



The SEM images taken from the fractured surface of SiC-coated and uncoated diamond/Al composites are shown in Fig. 5. The surface of the diamond particles was continuously covered by the interfacial reaction product. As seen from the Raman spectra in Fig. 6, all the peaks belong to  $\text{Al}_4\text{C}_3$  phase [12, 30]. Therefore, the reaction product was determined to be  $\text{Al}_4\text{C}_3$ . Also, the presence of  $\text{Al}_4\text{C}_3$  interphase on SiC-coated diamond particles proved that the reaction, given in Eq. (3), spontaneously proceeds, despite the predictions according to thermodynamic calculations. Although the composites were fabricated with the same parameters, the  $\text{Al}_4\text{C}_3$  interphases are coarser and higher amounts on the uncoated diamond particles than on those of the SiC coated, as shown in Figs. 5d, e and 6. It indicates that the SiC coating of diamond particles suppresses the formation of  $\text{Al}_4\text{C}_3$  at the interface during the fabrication process. These results are in good agreement with the TC results of composites. While the  $\text{Al}_4\text{C}_3$  interphase contributes to TC by chemically bonding diamond particles and Al matrix, excess amounts of  $\text{Al}_4\text{C}_3$  act as a thermal barrier at the interface, due to its low thermal conductance. Therefore, the SiC-coated diamond/Al composite with low content  $\text{Al}_4\text{C}_3$  has higher TC ( $528 \text{ W/m}\cdot\text{K}$ ) than uncoated diamond/Al composite ( $376 \text{ W/m}\cdot\text{K}$ ).

The thermal durability test results are shown in Fig. 7a and b. The results are consistent with the  $\Delta G_T$  values of the reactions presented in Table 1. Because the Al-SiC reaction (Eq. 3) had positive  $\Delta G_T$  values below the melting point of Al, the  $\text{Al}_4\text{C}_3$  interphase is not thermodynamically stable. Therefore, the TC of SiC-coated diamond/Al composite remained stable up to  $500 \text{ }^\circ\text{C}$  even for 120 h. On the other hand, solid Al and C are thermodynamically incompatible (*i.e.*, reactive), due to the negative  $\Delta G_T$  values. When the uncoated diamond/Al composite was exposed to elevated temperature, the  $\text{Al}_4\text{C}_3$  became large, as shown in Fig. 5f. So, the initial TC value decreased

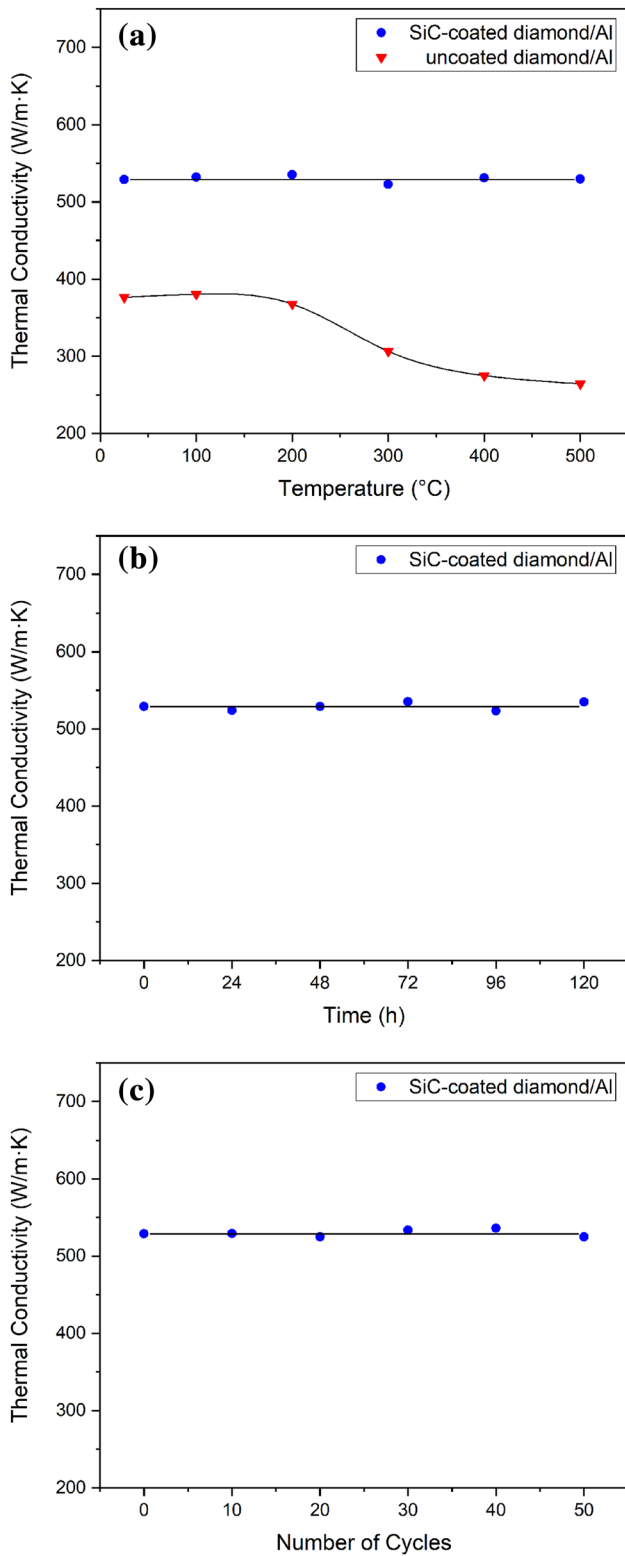


**Figure 7** **a** Temperature-dependent thermal durability test results of the composites, **b** time-dependent thermal durability test results of the SiC-coated diamond/Al composite at 500 °C and **c** thermal shock test results of the SiC-coated diamond/Al composite between 300 °C and room temperature.

dramatically, due to the low TC of  $Al_4C_3$ . When the thickness of  $Al_4C_3$  interphase increased, carbon diffusion from diamond to Al becomes difficult, and the TC displayed exponential decay despite the increasing temperature. Also, the TC stability of the coated diamond/Al composite indicated that the diamond particles were conformally coated with SiC. Otherwise, the Al-C reaction would occur on the uncoated parts of the diamond particles, and the TC would decrease because of  $Al_4C_3$  formation.

As shown in Fig. 7.c, the SiC-coated diamond/Al composite maintained its TC value during 50 thermal cycles between 300 °C and room temperature. This result indicated that the diamond particle–Al matrix interfaces were not separated from each other. Two mechanisms contributed to TC stability during thermal shock. Firstly, chemically bonding across the diamond/SiC/ $Al_4C_3$ /Al interfaces strengthened the adhesion between the diamond particles and the Al matrix. Secondly, since the CTEs of SiC and  $Al_4C_3$  are between those of diamond and Al, a gradual CTE transition from diamond particle to Al was built-in (CTEs of diamond, SiC,  $Al_4C_3$ , Al are 1, 3, 8, 23 ppm/K, respectively [1, 5, 31]). As a result of both contributing mechanisms, the effect of compressive and tensile stresses acting on the interfaces decreased.

Diamond/Al composites are moisture-sensitive due to the hygroscopic nature of the  $Al_4C_3$  phase. Hydrolysis of  $Al_4C_3$  in water occurred according to the reaction given in Eq. (4) [14]. The wet environment durability test results of the composites are shown in Fig. 8. While the SiC-coated diamond/Al

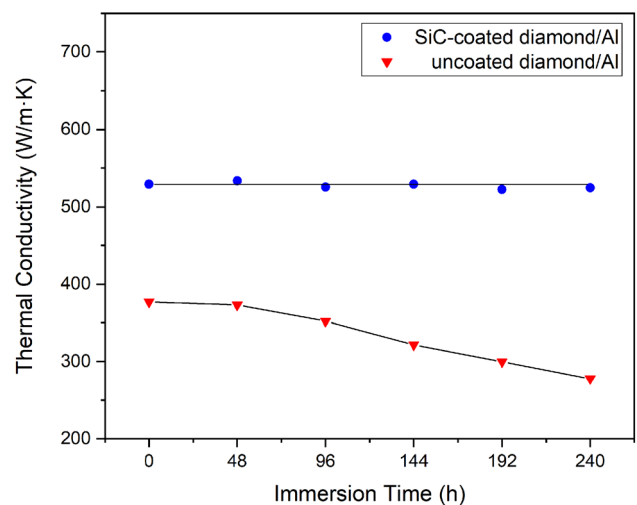
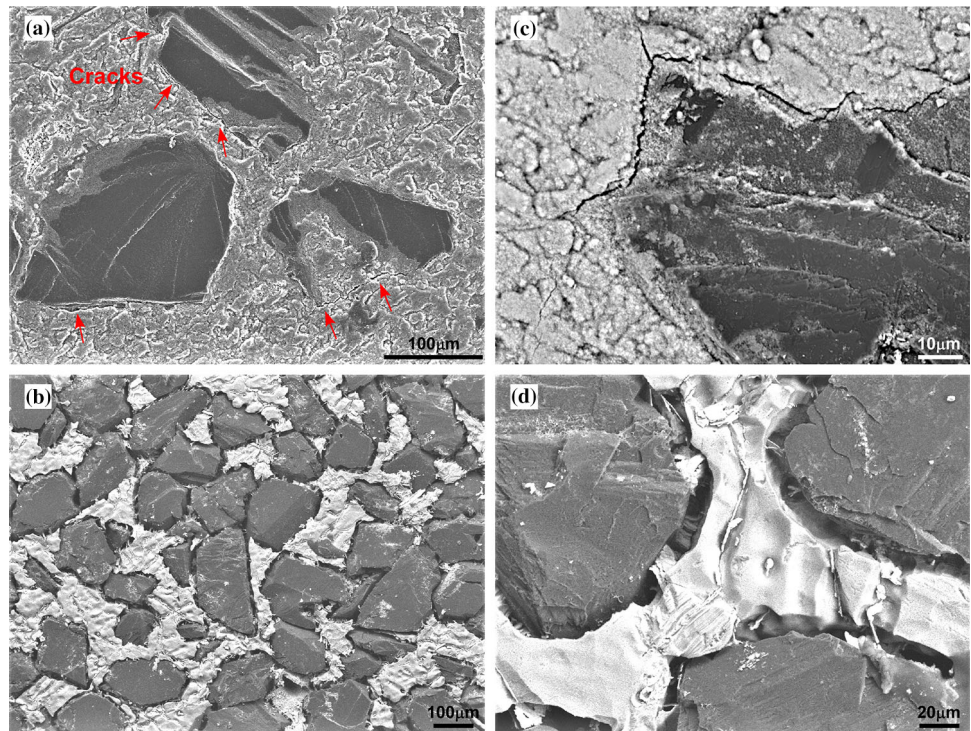


**Figure 8** Wet environment durability test results of the composites.

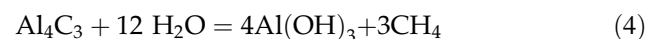


**Figure 9** Surface SEM images of the uncoated diamond/Al composite after the wet environment durability test: **a** before, **b** after the aluminum hydroxides were selectively dissolved. **c**, **d** high magnification of **a**, **b**, respectively.



composite maintained its TC value in distilled water at room temperature during 240 h, the TC of the uncoated diamond/Al composite decreased under the same conditions, due to its higher content of  $\text{Al}_4\text{C}_3$  interphase. The decomposition of  $\text{Al}_4\text{C}_3$  into porous aluminum hydroxides led to a large volume expansion [32, 33]. The stresses, caused by the increase in volume, induced crack formation at the interface, as shown in Fig. 9a and c. Consequently, the gaps formed decreased the TC value dramatically. The cracks could also be observed in the Al matrix. This result showed that degradation was not limited to the interface. After the wet environment durability test of the uncoated diamond/Al composite, the aluminum hydroxides were selectively dissolved in a solution containing 6%  $\text{H}_3\text{PO}_4$  and 1.8%  $\text{H}_2\text{CrO}_4$ . As shown in Fig. 9b and d, the large gaps indicated that in addition to  $\text{Al}_4\text{C}_3$ , the Al matrix also had hydrolyzed into aluminum hydroxides. This result is consistent with a study reporting that the thickness of aluminum hydroxide increases during 510 days [33]. The degradation of the Al matrix can be explained by the crevice corrosion mechanism. Crevice corrosion is initiated by changes in local chemistry within the cavity. Water penetrates through the cracks resulting from  $\text{Al}_4\text{C}_3$  hydrolysis, and the environment in the cavity creates the

conditions necessary for the initiation and propagation of crevice corrosion. After the aluminum hydroxides were selectively dissolved, the composite thickness was significantly reduced by the dropping of diamond particles detached from the matrix. It demonstrated that crevice corrosion caused degradation to propagate inward from the surface of the composite. Therefore, if the composite continued to be exposed to moisture, its TC will decrease further over time. Since the SiC-coated diamond/Al composite consisted of lower amounts of  $\text{Al}_4\text{C}_3$  interphase, its TC remained stable in distilled water under the test conditions. However, a decrease in TC of SiC-coated diamond/Al composite was inevitable, due to its  $\text{Al}_4\text{C}_3$  content. The low amount of  $\text{Al}_4\text{C}_3$  delayed initiation of the hydrolysis reaction.



## Conclusions

Diamond/Al composites were fabricated by use of gas pressure infiltration. The results showed that the SiC-coated diamond particles suppressed  $\text{Al}_4\text{C}_3$  interphase formation during fabrication, which was consistent with SiC-coated diamond/Al composites

exhibiting higher TC (528 W/m·K) than uncoated diamond/Al composite (376 W/m·K). When these TC results are evaluated together with the literature, it is clear that the significantly higher TC value was due to controlling the amount of  $\text{Al}_4\text{C}_3$  via SiC coating, despite using low-quality diamond particles. It indicated that the effect of diamond quality on TC was minimized, by suppressing  $\text{Al}_4\text{C}_3$  formation during fabrication. The CTE of SiC-coated diamond/Al composite was obtained as 7.2 ppm/K at room temperature.

Unlike the uncoated diamond/Al composite, the SiC-coated diamond/Al composite exhibited long-term stability up to 500 °C, as the Al-C reaction was prevented by conformal SiC coating of the diamond particles, and it showed considerably higher moisture resistance during 240 h. Also, the SiC coating of diamond particles contributed to the resistance of the composite against thermal shock between 300 °C and room temperature.

As a consequence, this study demonstrates that SiC-coated diamond/Al composites are promising material candidates for advanced thermal management even under extreme conditions.

## Acknowledgements

The authors would like to express their gratitude to Dr. Cleve Ow-Yang, Dr. Mustafa Ürgen and Dr. Kay Weidenmann for their contributions.

## Funding

This work was supported by Research Fund of the Istanbul Technical University. Project Number MOA-2019-42309.

## Declarations

**Conflict of interest** The authors declare that they have no conflict of interest.

## References

- Zweben C (2005) Ultrahigh-thermal-conductivity packaging materials. In: 21st IEEE semiconductor thermal measurement and management symposium, pp 168–174
- Timbs K, Khatamifar M, Antunes E, Lin W (2021) Experimental study on the heat dissipation performance of straight and oblique fin heat sinks made of thermal conductive composite polymers. *Therm Sci Eng Prog* 22:100848. <https://doi.org/10.1016/j.tsep.2021.100848>
- Kitzmantel M, Neubauer E (2015) Innovative hybrid heat sink materials with high thermal conductivities and tailored CTE. In: Proceedings of SPIE—the international society for optical engineering
- Yamamoto Y, Imai T, Tanabe K et al (1997) The measurement of thermal properties of diamond. *Diam Relat Mater* 6:1057–1061. [https://doi.org/10.1016/s0925-9635\(96\)00772-8](https://doi.org/10.1016/s0925-9635(96)00772-8)
- Jacobson P, Stoupin S (2019) Thermal expansion coefficient of diamond in a wide temperature range. *Diam Relat Mater* 97:107469. <https://doi.org/10.1016/j.diamond.2019.107469>
- Weber L, Tavangar R (2009) Diamond-based metal matrix composites for thermal management made by liquid metal infiltration—potential and limits. *Adv Mater Res* 59:111–115. <https://doi.org/10.4028/www.scientific.net/amr.59.111>
- Monje IE, Louis E, Molina JM (2014) On critical aspects of infiltrated Al/diamond composites for thermal management: diamond quality versus processing conditions. *Compos Part A Appl Sci Manuf* 67:70–76. <https://doi.org/10.1016/j.compositesa.2014.08.015>
- Xue C, Yu JK (2013) Enhanced thermal conductivity in diamond/aluminum composites: comparison between the methods of adding Ti into Al matrix and coating Ti onto diamond surface. *Surf Coatings Technol* 217:46–50. <https://doi.org/10.1016/j.surfcoat.2012.11.070>
- Edtmaier C, Segl J, Rosenberg E et al (2018) Microstructural characterization and quantitative analysis of the interfacial carbides in Al(Si)/diamond composites. *J Mater Sci* 53:15514–15529. <https://doi.org/10.1007/s10853-018-2734-1>
- Che Z, Wang Q, Wang L et al (2017) Interfacial structure evolution of Ti-coated diamond particle reinforced Al matrix composite produced by gas pressure infiltration. *Compos Part B Eng* 113:285–290. <https://doi.org/10.1016/j.compositesb.2017.01.047>
- Li X, Yang W, Sang J et al (2020) Low-temperature synthesizing SiC on diamond surface and its improving effects on thermal conductivity and stability of diamond/Al composites. *J Alloys Compd* 846:156258. <https://doi.org/10.1016/j.jallcom.2020.156258>
- Monje IE, Louis E, Molina JM (2016) Role of  $\text{Al}_4\text{C}_3$  on the stability of the thermal conductivity of Al/diamond composites subjected to constant or oscillating temperature in a

- humid environment. *J Mater Sci* 51:8027–8036. <https://doi.org/10.1007/s10853-016-0072-8>
- [13] Ruch PW, Beffort O, Kleiner S et al (2006) Selective interfacial bonding in Al(Si)-diamond composites and its effect on thermal conductivity. *Compos Sci Technol* 66:2677–2685. <https://doi.org/10.1016/j.compscitech.2006.03.016>
- [14] Lu Y, Wang X, Zhang Y et al (2018) Aluminum carbide hydrolysis induced degradation of thermal conductivity and tensile strength in diamond/aluminum composite. *J Compos Mater* 52:2709–2717. <https://doi.org/10.1177/0021998317752504>
- [15] Tan Z, Li Z, Fan G et al (2013) Fabrication of diamond/aluminum composites by vacuum hot pressing: process optimization and thermal properties. *Compos Part B Eng* 47:173–180. <https://doi.org/10.1016/j.compositesb.2012.11.014>
- [16] Monje IE, Louis E, Molina JM (2013) Optimizing thermal conductivity in gas-pressure infiltrated aluminum/diamond composites by precise processing control. *Compos Part A Appl Sci Manuf* 48:9–14. <https://doi.org/10.1016/j.compositesa.2012.12.010>
- [17] Zhang Y, Li J, Zhao L, Wang X (2015) Optimisation of high thermal conductivity Al/diamond composites produced by gas pressure infiltration by controlling infiltration temperature and pressure. *J Mater Sci* 50:688–696. <https://doi.org/10.1007/s10853-014-8628-y>
- [18] Mizuuchi K, Inoue K, Agari Y et al (2011) Processing of diamond particle dispersed aluminum matrix composites in continuous solid-liquid co-existent state by SPS and their thermal properties. *Compos Part B Eng* 42:825–831. <https://doi.org/10.1016/j.compositesb.2011.01.012>
- [19] Guo C, He X, Ren S, Qu X (2016) Effect of (0–40) wt. % Si addition to Al on the thermal conductivity and thermal expansion of diamond/Al composites by pressure infiltration. *J Alloys Compd* 664:777–783. <https://doi.org/10.1016/j.jallcom.2015.12.255>
- [20] Johnson WB, Sonuparlak B (1993) Diamond/Al metal matrix composites formed by the pressureless metal infiltration process. *J Mater Res* 8:1169–1173. <https://doi.org/10.1557/JMR.1993.1169>
- [21] Li N, Wang L, Dai J et al (2019) Interfacial products and thermal conductivity of diamond/Al composites reinforced with ZrC-coated diamond particles. *Diam Relat Mater* 100:107565. <https://doi.org/10.1016/j.diamond.2019.107565>
- [22] Che Z, Li J, Wang Q et al (2018) The formation of atomic-level interfacial layer and its effect on thermal conductivity of W-coated diamond particles reinforced Al matrix composites. *Compos Part A Appl Sci Manuf* 107:164–170. <https://doi.org/10.1016/j.compositesa.2018.01.002>
- [23] Carotenuto G, Gallo A, Nicolais L (1994) Degradation of SiC particles in aluminium-based composites. *J Mater Sci* 29:4967–4974. <https://doi.org/10.1007/BF01151086>
- [24] Bartuli C, Carassiti F, Valente T (1994) Interfacial reactions in Al/SiC composites produced by low pressure plasma spray. *Adv Perform Mater* 1:231–242. <https://doi.org/10.1007/BF00711205>
- [25] Miyamoto Y, Lin J, Yamashita Y et al (2000) Reactive coating of SiC on diamond particles. In: 24th annual conference on composites, advanced ceramics. *Mater Struct B* 185–192
- [26] Hutsch T, Schubert T, Schmidt J, et al (2010) Innovative metal-graphite composites as thermally conducting materials. In: World PM 2010 proceedings of the world powder metallurgy congress and exhibition
- [27] Yang W, Peng K, Zhu J et al (2014) Enhanced thermal conductivity and stability of diamond/aluminum composite by introduction of carbide interface layer. *Diam Relat Mater* 46:35–41. <https://doi.org/10.1016/j.diamond.2014.04.007>
- [28] Malcolm C (1998) NIST-JANAF Thermochemical Tables. *J Phys Chem Ref Data*
- [29] Iseki T, Maruyama T, Kameda T (1984) Interfacial reactions between SiC and aluminium during joining. *J Mater Sci* 19:1692–1698
- [30] Kennedy JL, Drysdale TD, Gregory DH (2015) Rapid, energy-efficient synthesis of the layered carbide, Al<sub>4</sub>C<sub>3</sub>. *Green Chem* 17:285–290. <https://doi.org/10.1039/c4gc01277a>
- [31] Asthana R, Tewari SN (1993) Interfacial and capillary phenomena in solidification processing of metal-matrix composites. *Compos Manuf* 4:3–25. [https://doi.org/10.1016/0956-7143\(93\)90012-W](https://doi.org/10.1016/0956-7143(93)90012-W)
- [32] Li Y, Ke C, Zhang Y et al (2014) Study on erosion mechanism of Cr<sub>2</sub>O<sub>3</sub>-Al<sub>2</sub>O<sub>3</sub>-ZrO<sub>2</sub> bricks for coal-water slurry pressurized gasifier. In: Goski DG, Smith JD (eds) Proceedings of the unified international technical conference on refractories (UNITECR 2013), pp 1223–1227
- [33] Rodríguez-Reyes M, Pech-Canul MI, Parga-Torres JR et al (2011) Development of aluminum hydroxides in Al-Mg-Si/SiCp in infiltrated composites exposed to moist air. *Ceram Int* 37:2719–2722. <https://doi.org/10.1016/j.ceramint.2011.04.028>

**Publisher's Note** Springer Nature remains neutral with regard to jurisdictional claims in published maps and institutional affiliations.